Bacterial Structural Genomics Target Enabled by Recently Discovered Potent Fungal ACS Inhibitor

Authors

Nicholas D. DeBouver [a,b], Madison J. Bolejack [a,b], Taiwo E. Esan [c], Damian J. Krysan [d], Timothy J. Hagen [c], Jan Abendroth [a,b]

[a] UCB Pharma, 7869 NE Day Road West, Bainbridge Island, WA, 98110, USA

[b] Seattle Structural Genomics Center for Infectious Disease (SSGCID), Seattle, WA 98109, USA

[c] Chemistry and Biochemistry, Northern Illinois University, 1426 Lincoln Hwy, DeKalb, IL, 60115, USA

[d] Microbiology/Immunology, Carver College of Medicine, University of Iowa, Iowa City, Iowa, 52242, United States

Correspondence email: jan.abendroth@ucb.com

Synopsis Rescue efforts for ACS1 proteins in complex with ethyl-AMP yielded the first structure from *L. pneumophila* with a very well-defined ethyl-AMP bound in the active site.

Abstract The compound ethyl-adenosyl monophosphate ester (ethyl-AMP) has been shown to effectively inhibit Acetyl CoA synthase (ACS) enzymes and to facilitate the crystallization of fungal ACS enzymes in various contexts. In this study, the addition of ethyl-AMP to a bacterial ACS from *Legionella pneumophila* resulted in successful co-crystal structure determination of a target structure which had previously eluded researchers. The ability of ethyl-AMP to inhibit ACS enzymes and to facilitate crystallization makes it a valuable tool in structural studies of this class of proteins.

1. Introduction

In the 1980s, the respiratory pathogen known as *Legionella pneumophila* caused numerous outbreaks of a severe form of pneumonia called Legionnaire's disease in healthcare centers. Even today, this disease continues to have a high mortality rate among vulnerable populations, including the elderly, infants, and individuals with underlying health conditions (Chanin and Opal, 2017). While there are more than 50 species of Legionella, *L. pneumophila* is responsible for 80% of cases of Legionnaire's disease globally (Chanin and Opal, 2013).

Enzymes called acetyl-coenzyme A synthetases (ACSs) play a crucial role in the synthesis of acetyl-CoA, a molecule involved in the tricarboxylic acid (TCA) cycle and are vital for the central carbon

and energy metabolism of both prokaryotes and eukaryotes. Inhibiting ACS enzymes has shown promise in terms of exhibiting antifungal and anti-tumor activity in eukaryotes, and it is possible that similar effects may be observed in bacteria such as *L. pneumophila*.

The mission of the Seattle Structural Genomics Center for Infectious Disease (SSGCID, ssgcid.org) is the determination of atomic structures of proteins with an important role in human pathogens. Pathogens include NIAID Category A-C agents as well as emerging and re-emerging infectious disease organisms. In order to increase success rates, crystallization experiments are executed with both apo proteins and with known ligands, such as co-factors, substrates, products and inhibitors. Since the ACS1 inhibitor ethyl AMP had been successfully used for crystallizing fungal ACS proteins (Jezewski et al, 2021), and apo *L. pneumophila* did not crystallize, we attempted to crystallize *L. pneumophila* ACS1 in the presence of the fungal ACS1 inhibitor. Here, we report the 2.4Å structure of *L. pneumophila* ACS1 in complex with ethyl-AMP.

2. Materials and methods

2.1. Macromolecule production

Cloning of Expression Constructs.

The gene for *L. pneumophila* ACS1 was amplified from genomic DNA and cloned into the expression vector pBG1861 using ligand-independent cloninghttps://www.ncbi.nlm.nih.gov/pmc/articles/PMC6416309/ (Aslanidis et al, 1990). The expression vector provides a non-cleavable N-terminal His_6-tag (SSGCID target ID LepnA.00629.a, SSGCID construct ID LepnA.00629.a.B1, SSGCID batch LepnA.00629.a.B1.PW38314). *L. pneumophila* ACS1 was expressed in *E. coli* BL21(DE3) Rosetta Oxfords following standard SSGCID protocols as described previously https://www.ncbi.nlm.nih.gov/pmc/articles/PMC6416309/ (Choi et al, 2011). Purification was done using Ni-NTA affinity and size exclusion chromatography following standard SSGCID protocols (Bryan et al, 2011). The purified protein was concentrated to 33.45 mg/ml in its final buffer (25 mM HEPES pH 7.0, 500 mM NaCl, 5% glycerol, 2 mM DTT, 0.025% NaN_3), flash frozen in liquid nitrogen and stored at −80 °C.

Table 1 Macromolecule production information

In the primers, indicate any restriction sites, cleavage sites or introduction of additional residues, *e.g.* His6-tag, as well as modifications, *e.g.* Se-Met instead of Met.

Source organism	*Legionella pneumophila subsp. pneumophila* (strain Philadelphia 1 / ATCC 33152 / DSM 7513) (strain: Philadelphia 1 / ATCC 33152 / DSM 7513); Uniprot ID Q5ZZ84

DNA source	Legionella pneumophila Philadelphia 1 / ATCC 33152
Forward primer	CTCACCACCACCACCACCATATGCTTCCCGTTCATCTAAAGCAC
Reverse primer	ATCCTATCTTACTCACTTACCGCTTCAAAATATTTTTCATGAGTT
Cloning vector	BG1861
Expression vector	BG1861
Expression host	BL 21 (DE3) Rosetta Oxfords
Complete amino acid sequence of the construct produced	MAHHHHHHMLPVHLKHPHLTATEEYLSEFW SEIAAQTIDWIQPWSITLQGGLHKGDVKWFQ GGLLNVSANCLDRHLPHKA NQTAIIWEGDDENQNKTLTFAQLYSEVCKM SNVLKSLNVRRGDTVGIYLPMIPEAAIAMLA CARIGAIHTVVFAGFSAHA LQQRLIASSCKCLITADAFQRGGKTIPLKK QADEASVDLNITKLVVKNSNAPTALNKNKEH WWHELKQTVSDQCTPEPMN TEDPLFILYTSGSTGQPKGVVHTTGGYLVQ AAYTHQLIFACQDNEVFWCTADVGWITGHSY VVYGPLCNGITTLMFEGIP TWPDAARNWRIIDKHQVNVFYTAPTAIRSL MRAGDQWLNSSSRSSLRLLGSVGEPINPEAW NWYHQKVGQGKCPIVDTWW QTETGAIMISPRASDEVIKPGSARKPIPGI VPLLLNEQGHEINGAGEGLLAIKYPWPSMAR TIAGDHQRYCNTYLSNGYY ITGDGAKRDEDGDYWITGRIDDVLNVSGHR LGTAEIESALVSHPKVAEAGVVGIPHDLKGQ AIFAYVILKQGNKPDAELQ TELMERVKDQISAIAKPDVIQFANDLPKTR SGKIMRRILRKIACKEVSHIDELGDLTTLAN PQIVEELMKNILKR

2.2. Crystallization

Crystals of ACS1 from *L. pneumophila* in complex with adenosine-5'-ethylphosphate (ethyl-AMP) were grown by mixing 0.4 µL protein at 20 mg/mL, supplemented with 2mM TCEP and 3mM ethyl AMP, with 0.4 µL reservoir of sparse matrix screen JCSG Top96 (Rigaku Reagents), condition B6 (100mM HEPES free acid / sodium hydroxide pH 7.5, 20% (w/V) PEG 4000, 20% (V/V) 2-propanol), in MRC2 sitting drop crystallization trays (SwisSci) with 50 µL reservoir volume. The

crystals were cryoprotected with a mix of 20% (V/V) ethylene glycol + 3mM compound with the reservoir solution. Crystals were then vitrified in liquid nitrogen.

Table 2 Crystallization

Method	Vapor diffusion, sitting drop
Plate type	MRC2
Temperature (K)	287
Protein concentration	20 mg/mL
Buffer composition of protein solution	25 mM HEPES pH 7.0, 500 mM NaCl, 5% Glycerol, 2 mM DTT, and 0.025% Azide
Composition of reservoir solution	100mM HEPES free acid / sodium hydroxide pH 7.5, 20% (w/v) PEG 4000, 20% (v/v) 2-propanol
Volume and ratio of drop	0.4 µL : 0.4 µL
Volume of reservoir	50 µL

2.3. Data collection and processing

X-ray diffraction data were collected at the APS beamline 21-ID-F on a Rayonix MX-300 CCD detector. Data were processed and reduced with XDS/XSCALE (Kabsch, 2010) to 2.4Å resolution, based on standard criteria for SSGCID and its partner center CSGID (https://csgid.org/pages/sg_metrics).

Table 3 Data collection and processing

Values for the outer shell are given in parentheses.

Diffraction source	APS beamline 21-ID-F
Wavelength (Å)	0.97872
Temperature (K)	100
Detector	Rayonix MX-300 CCD
Crystal-detector distance (mm)	300mm
Rotation range per image (°)	1
Total rotation range (°)	100
Exposure time per image (s)	1.25
Space group	$P4_12_12$
a, *b*, *c* (Å)	74.93, 74.93, 228.79
α, β, γ (°)	90, 90, 90

Mosaicity (°)	0.121
Resolution range (Å)	50–2.40 (2.46–2.40)
Total No. of reflections	207,2415 (15,561)
No. of unique reflections	26,436 (1908)
Completeness (%)	99.5 (100)
Redundancy	7.8 (8.2)
$\langle I/\sigma(I)\rangle$	20.74 (4.42) (**see note below #**)
$R_{r.i.m.}$	0.069 (0.662)
Overall *B* factor from Wilson plot (Å^2)	53.1 **see note below †**

If mean $I/\sigma(I)$ in outer shell is <2.0, please provide an explanation [as a footnote here] and provide resolution at which it falls below 2.0.

† State here if there are any anomalies in the Wilson plot, such as spikes arising from ice rings, *etc.*

2.4. Structure solution and refinement

The structure solved by molecular replacement using MoRDa (Vagin, Lebedev, 2015) (PDB ID: 1PG4 (Gulick et al, 2003)) Iterative manual model building using COOT (Emsley et al, 2010) and phenix.refine (Adams et al, 2010) continued until R and Rfree converged. Model quality was validated using COOT and MolProbity (Chen et al, 2010) prior to deposition in the Protein Data Bank with accession code 7mmz (See Table 4). Diffraction images are available on Integrated Resource for Reproducibility in Macromolecular Crystallography (http://www.proteindiffraction.org, (Grabowski et al, 2016)

Table 4 Structure solution and refinement

Values for the outer shell are given in parentheses.

Resolution range (Å)	45.47–2.40 (2.46–2.40)
Completeness (%)	99.6
σ cutoff	$F > 1.35\sigma(F)$
No. of reflections, working set	26,362 (1561)
No. of reflections, test set	2041 (150)
Final R_{cryst}	0.188 (0.243)
Final R_{free}	0.225 (0.265)
Cruickshank DPI	0.220

No. of non-H atoms	
Protein	4214
Ligand	29
Water	122
Total	4365
R.m.s. deviations	
Bonds (Å)	0.006
Angles (°)	0.757
Average *B* factors (Å^2)	
Protein	55.1
Ligand	36.8
Water	50.0
Ramachandran plot	
Most favoured (%)	96.4
Allowed (%)	3.6

3. Results and discussion

L. pneumophila ACS crystallizes with one molecule per asymmetric unit. The structure (Figure 2) refines well with R_{work}=0.188 and R_{free}=0.225 and a MolProbity score of 1.20. There is adequate density throughout the chain. Only for the N-terminal eleven residues plus His-tag, a disordered loop between Lys 542 and Lys 546, and for the C-terminal 52 residues (past Ala 575), the density is too weak to build a model with confidence. Clear density allowed for modelling of ethyl-AMP.

ACS proteins consist of two domains, the N-terminal ATP-binding domain and the C-terminal domain. The latter undergoes a very significant rotation between the two reaction steps, the adenylation reaction (AD-conf) and the thioesterification reaction (TE-conf) (Jezewski et al, 2021)(Gulick, 2009). *L. pneumophila* ACS shares the same two domain fold as other bacterial or fungal ACS in complex with adenosine-phosphate and analogs with overall RMDS of around 1Å RMSD per PDBeFOLD analysis (Krissinel and Henrick, 2004). As seen in other adenosine-ligand bound ACS structures (Jezewski et al, 2021),the CTD has undergone a 140-degree rotation upon the binding event of ATP as outlined in our previous paper (Jezewski et al, 2021).The hypothesis is that

binding to ethyl-AMP locks into this intermediate conformation which allows it to crystallize more readily.

As anticipated from the multiple sequence alignment with fungal ACS (Figure 1), the residues of *L. pneumophila* ACS that interact with ethyl-AMP are conserved, see Figure 3. The sequence identity between *L. pneumophila* ACS and previously crystallized fungal ACS constructs is rather moderate (~45%). However, the residues that interact with the inhibitor ethyl AMP in the fungal structures are highly conserved in the *L. pneumophila* protein as well, see Figure 2. We therefore attempted to crystallize *L. pneumophila* ACS1, which had not crystallized as apo protein, in the presence of ethyl AMP. Our hypothesis was confirmed: *L. pneumophila* ACS1 crystallized in complex with the fungal ACS1 inhibitor and engages in very similar interactions with the compound as fungal ACS1. The homology extends to Trp 392, a conserved Trp residue which has shown to impact substrate specificity via the so called Trp wall (Jezewski et al, 2021).

Our results demonstrate that ethyl-AMP has facilitated the crystallization of ACS from *L. pneumophila*. This might make ethyl-AMP a valuable tool for structural biology of other ACSs. Moreover, this study exemplifies that next to co-factors, substrates and products, inhibitors of homologs with moderate sequence identity can be a very helpful tool.

Acknowledgements The acknowledgements should be in a single paragraph [Style: IUCr acknowledgements]

SSGCID is funded by federal funds from the National Institute of Allergy and Infectious Diseases (NIAID), National Institutes of Health (NIH), Department of Health and Human Services, under contract no. HHSN272201700059C from September 1, 2017.

APS/LS-CAT research used resources of the Advanced Photon Source, a U.S. Department of Energy (DOE), Office of Science user facility operated for the DOE Office of Science by Argonne National Laboratory under contract no. DE-AC02- 06CH11357. Use of LS-CAT Sector 21 was supported by the Michigan Economic Development Corporation and the Michigan Technology Tri-Corridor (Grant 085P1000817).

Work on the ACS1 inhibitor project and synthesis and of ethyl-AMP was supported by NIH grant 1R01AI161973.

Purchase of the NMR spectrometer used to characterize the ethylAMP in this publication was supported by the National Science Foundation under the MRI award CHE-2117776.

Figures:

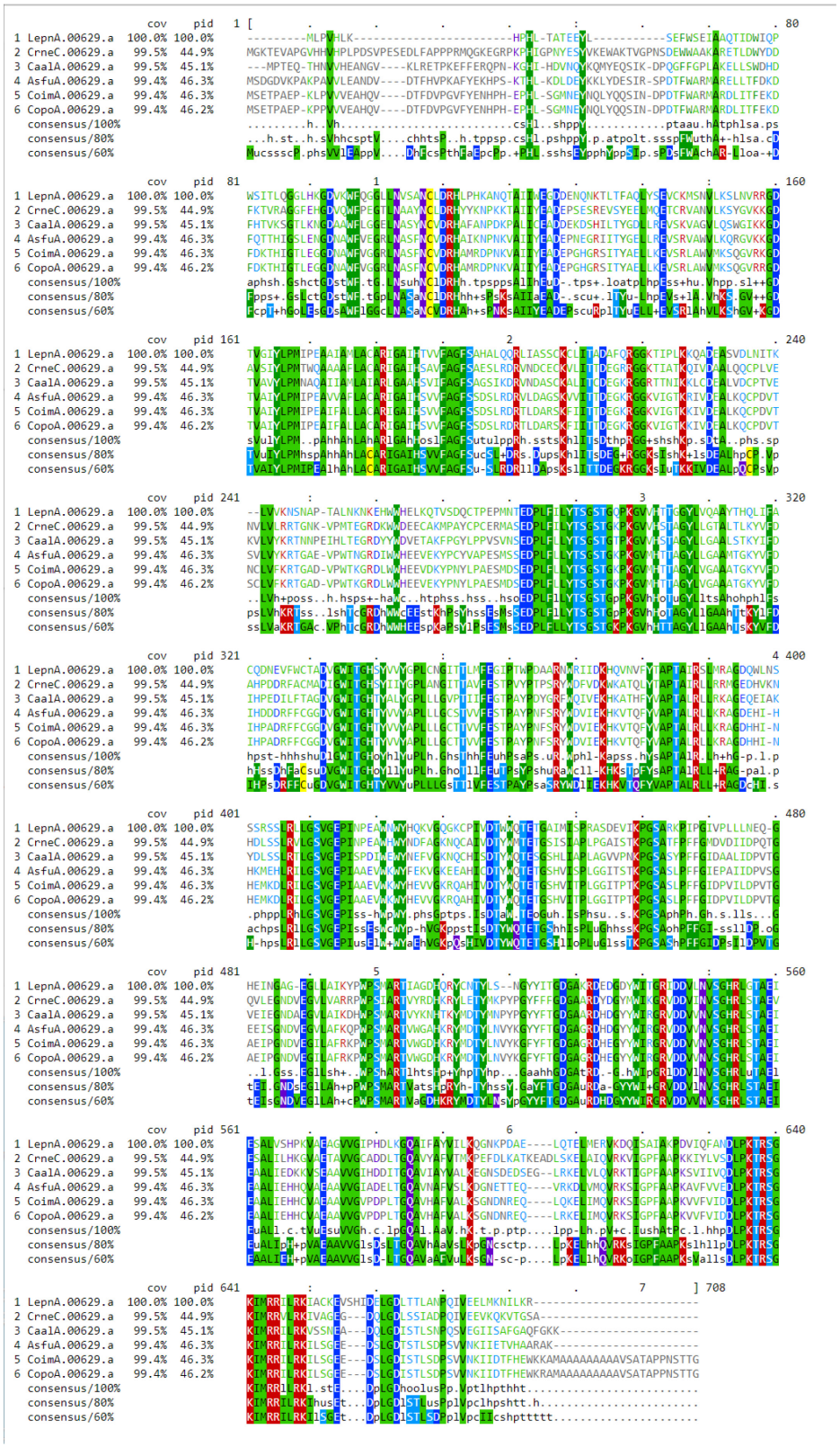

out_01.html

Figure 1. MSA generated using the MUSCLE algorithm (Edgar, 2021) of L. Pneumonia construct referenced against fungal ACSs previously crystallized with ethyl-AMP (Brown, 1998).

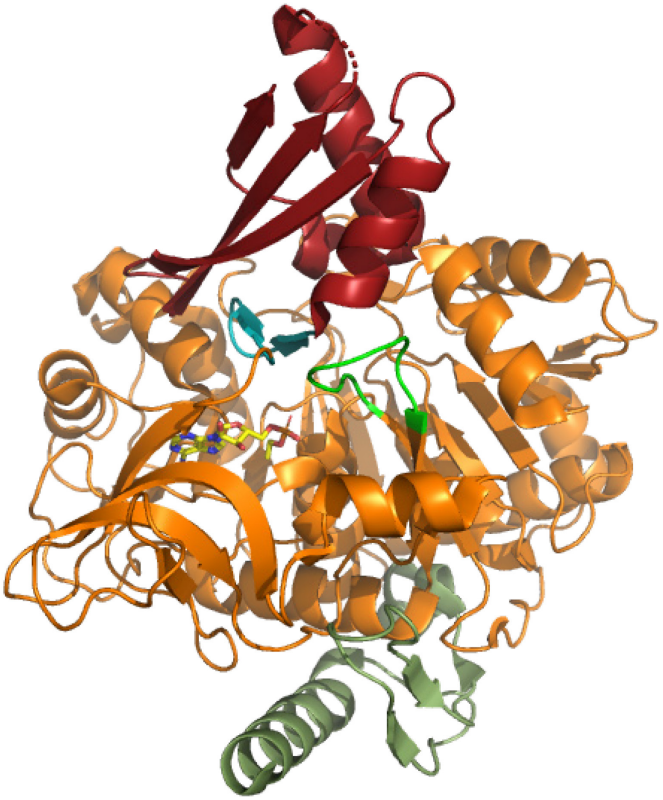

Figure 2: Structure of *L. pneumophila* ACS. Red indicates the CTD, Orange is the NTD, Dark green is the NT-Ext domain, cyan is the hinge region, lime green is the ATP-binding loop, yellow is bound ethyl-AMP. (Jezewski et al, 2021)

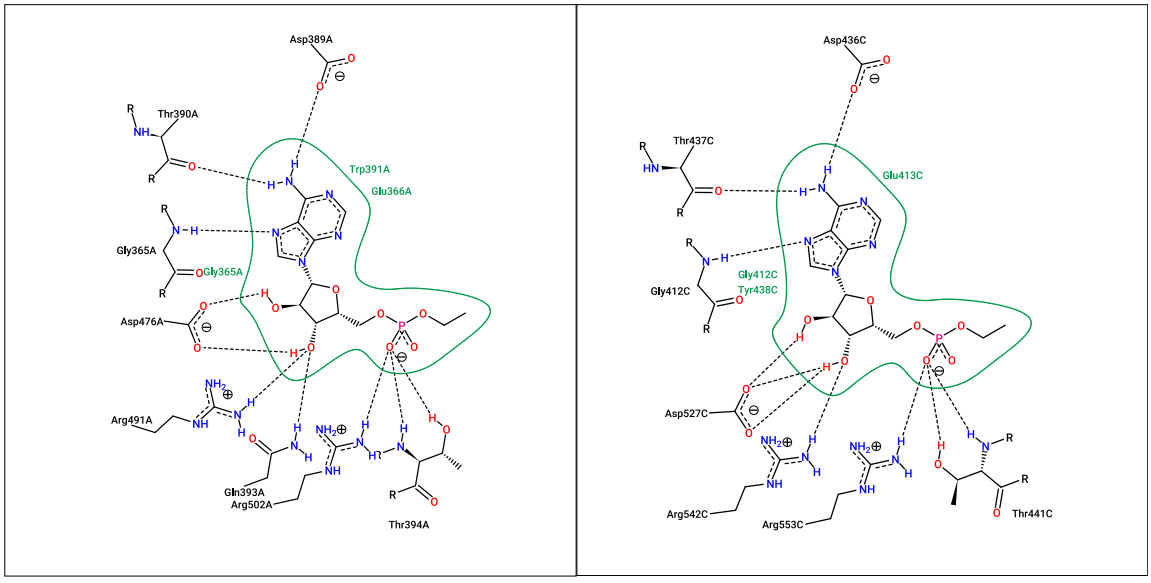

Figure 3

Sidechain interactions between (2a) *L. pneumophila* ACS and ethyl-AMP and (2b) *Cryptococcus neoformans* ACS (7KNO) and ethyl-AMP are highly conserved (Stierand et al, 2006) (Fricker et al, 2004).

References (IUCr style)

Ligand Binding diagrams - ZBH - Center for Bioinformatics protein plus server

Structure soln/refinement

In-text: authors' names followed immediately by the year of publication, *e.g.* Neder & Schulz (1998) or (Neder & Schulz, 1998). Where there are three or more authors, the reference in the text should be indicated in the form Smith *et al.* (1998) or (Smith *et al.*, 1998) *etc.*

Examples

Cowley, J. M. (1993). Editor. *Electron Diffraction Techniques*. Oxford University Press.

CRC Handbook of Chemistry and Physics (1983). 64th ed., edited by R. C. Weast, p. D-46. Boca Raton: CRC Press.

Cruickshank, D. W. J. (1998). *Acta Cryst*. A**54**, 687–696.

Author Surname, Author Initial. (Year Published). *Publication Title*. Volume number, Pages Used.

1. Adams, P.D., Afonine, P.V., Bunkóczi, G., Chen, V.B., Davis, I.W., Echols, N., Headd, J.J., Hung, L.W., Kapral, G.J., Grosse-Kunstleve, R.W. and McCoy, A.J. (2010) *PHENIX: a comprehensive Python-based system for macromolecular structure solution.* Acta Crystallographica Section D: Biological Crystallography. 66, 213-221.
2. Berman, H., Henrick, K. and Nakamura, H. (2003) *Announcing the worldwide protein data bank.* Nature Structural & Molecular Biology. 10, 980-980.
3. Berman, H.M., Westbrook, J., Feng, Z., Gilliland, G., Bhat, T.N., Weissig, H., Shindyalov, I.N. and Bourne, P.E. (2000) *The protein data bank.* Nucleic Acids Research. 28, 235-242.
4. Chahin, A. and Opal, S.M. (2017) *Severe Pneumonia Caused by Legionella pneumophila: Differential Diagnosis and Therapeutic Considerations*. Infectious Disease Clinics of North America. 31(1): 111-121.
5. Chen, V.B., Arendall, W.B., Headd, J.J., Keedy, D.A., Immormino, R.M., Kapral, G.J., Murray, L.W., Richardson, J.S. and Richardson, D.C. (2010) *MolProbity: all-atom structure S32 validation for macromolecular crystallography.* Acta Crystallographica Section D: Biological Crystallography. 66, 12-21.
6. Emsley, P., Lohkamp, B., Scott, W.G. and Cowtan, K. (2010) *Features and development of Coot.* Acta Crystallographica Section D: Biological Crystallography. 66, 486-501.
7. Fährrolfes, R., Bietz, S., Flachsenberg, F., Meyder, A., Nittinger, E., Otto, T., Volkamer, A., Rarey, M. (2017). *Nucleic Acids Research*. 45:W337-W343.
8. Fricker, P., Gastreich, M., and Rarey, M. (2004) *Automated Generation of Structural Molecular Formulas under Constraints.* Journal of Chemical Information and Computer Sciences, 44, 1065-1078.
9. Grabowski, M., Langner, K.M., Cymborowski, M., Porebski, P.J., Sroka, P., Zheng, H., Cooper, D.R., Zimmerman, M.D., Elsliger, M.A., Burley, S.K., and Minor, W. (2016) *A public database of macromolecular diffraction experiments*. Acta crystallographica Section D: Structural biology. 72 (Pt 11):1181-1193.
10. Grabowski, M., Cymborowski, M., Porebski, P.J., Osinski, T., Shabalin, I.G., Cooper, D.R., and Minor, W. (2019) *The Integrated Resource for Reproducibility in Macromolecular Crystallography: Experiences of the first four years.* Structural Dynamics. 6: 064301
11. Kabsch, W. (2010). *Xds.* Acta Crystallographica Section D: Biological Crystallography. 66,125-132.5.
12. Richards, A.M., Von Dwingelo, J.E., Price, C.T., and Kwaik, Y.A. (2013). *Cellular microbiology and molecular ecology of Legionella-amoeba interaction.* Virulence. 4(4): 307-314.
13. Schöning-Stierand, K., Diedrich, K., Fährrolfes, R., Flachsenberg, F., Meyder, A., Nittinger, E., Steinegger, R., Rarey, M. (2020). *Nucleic Acids Research.* 48:W48-W53.

14. Stierand, K., Maaß, P., Rarey, M. (2006) Molecular Complexes at a Glance: Automated Generation of two-dimensional Complex Diagrams. Bioinformatics, 22, 1710-1716.
15. Vagin, A. and Lebedev, A. (2015). *MoRDa, an automatic molecular replacement pipeline.* Acta Crystallographica Section A: Foundations and Advances. 71: s19.

REF:

LIC:

Aslanidis C, de Jong PJ. Ligation-independent cloning of PCR products (LIC-PCR) *Nucleic acids research.* 1990;**18**:6069–74. doi: 10.1093/nar/18.20.6069.

SSGCID-expression:

Choi R, et al. Immobilized metal-affinity chromatography protein-recovery screening is predictive of crystallographic structure success. *Acta crystallographica. Section F, Structural biology and crystallization communications.* 2011;**67**:998–1005. doi: 10.1107/S1744309111017374.

SSGCID-purification

Bryan CM, et al. High-throughput protein production and purification at the Seattle Structural Genomics Center for Infectious Disease. *Acta crystallographica. Section F, Structural biology and crystallization communications.* 2011;**67**:1010–4. doi: 10.1107/S1744309111018367.

XDS:

Kabsch W. XDS. *Acta crystallographica. Section D, Biological crystallography.* 2010;**66**:125–32. doi: 10.1107/S0907444909047337.

MORDA

A. Vagin and A. Lebedev. 2015. MoRDa, an automatic molecular replacement pipeline . Acta Crystallographica Section A: FOUNDATIONS AND ADVANCES. 71: s19.

1PG4

Gulick AM, Starai VJ, Horswill AR, Homick KM, Escalante-Semerena JC. The 1.75 A crystal structure of acetyl-CoA synthetase bound to adenosine-5'-propylphosphate and coenzyme A. Biochemistry. 2003 Mar 18;42(10):2866-73. doi: 10.1021/bi0271603. PMID: 12627952.

PROTEINDIFFRACTION

Grabowski M, Langner KM, Cymborowski M, Porebski PJ, Sroka P, Zheng H, Cooper DR, Zimmerman MD, Elsliger MA, Burley SK, Minor W (2016)
A public database of macromolecular diffraction experiments.
Acta crystallographica. Section D, Structural biology 72 (Pt 11):1181-1193. [Pub Med ID: 27841751] [Pub Med Central ID: PMC5108346]

PDBeFOLD

E. Krissinel and K. Henrick (2004). *Secondary-structure matching (SSM), a new tool for fast protein structure alignment in three dimensions*. *Acta Cryst.* D**60**, 2256---2268

PoseView

1. Stierand, K.; Maass, P. C.; Rarey, M., Molecular complexes at a glance: automated generation of two-dimensional complex diagrams. Bioinformatics 2006, 22 (14), 1710-6. DOI: https://doi.org/10.1093/bioinformatics/btl150

2. Fricker, P. C.; Gastreich, M.; Rarey, M., Automated drawing of structural molecular formulas under constraints. J Chem Inf Comput Sci 2004, 44 (3), 1065-78. DOI: https://doi.org/10.1021/ci049958u

MView – MSA Visualization
Brown, N.P., Leroy C., Sander C. (1998). MView: A Web compatible database search or multiple alignment viewer. *Bioinformatics*. **14** (4):380-381. [PubMed]
MView — MView (desmid.github.io)

MUSCLE – MSA algorithm
R.C. Edgar (2021) "MUSCLE v5 enables improved estimates of phylogenetic tree confidence by ensemble bootstrapping"
https://www.biorxiv.org/content/10.1101/2021.06.20.449169v1.full.pdf

Gulick:

Gulick, A. M. (2009) Conformational dynamics in the acylCoA synthetases, adenylation domains of non-ribosomal peptide synthetases, and firefly luciferase. ACS Chem. Biol. 4, 811−827.

Jezewski

Jezewski AJ, Alden KM, Esan TE, DeBouver ND, Abendroth J, Bullen JC, Calhoun BM, Potts KT, Murante DM, Hagen TJ, Fox D, Krysan DJ. Structural Characterization of the Reaction and Substrate Specificity Mechanisms of Pathogenic Fungal Acetyl-CoA Synthetases. ACS Chem Biol. 2021 Aug 20;16(8):1587-1599. doi: 10.1021/acschembio.1c00484. Epub 2021 Aug 9. PMID: 34369755; PMCID: PMC8383264.

Further information from SSGCID

Uniprot ID Q5ZZ84 - *Legionella pneumophila subsp. pneumophila (strain Philadelphia 1 / ATCC 33152 / DSM 7513)* - Acetyl-coenzyme A synthetase

Cloning vector: BG1861

LepnA.00629.a.B1.GE41429
harvested on: 4/5/2017
sequenced on: 4/27/2017
expected MW: 71kDa
observed MW: 71kDa
MW ratio: 1
antibiotic marker: ampicillin
expression colonies count: Good (10-50)
total expression level: Moderate Expression
soluble expression level: Moderate Expression
expression host: BL 21 (DE3) Rosetta

Purification

LepnA.00629.a.B1.PW38314
purified on: 7/17/2017
concentration: 33.45mg/ml
observed molecular weight: 69kDa
expression level: High Expression
protein purification buffer: 25 mM HEPES pH 7.0, 500 mM NaCl, 5% Glycerol, 2 mM DTT, and 0.025% Azide
expression host: BL 21 (DE3) Rosetta
vial count (approx.): 2
vial volume: 200µl

Final Buffer

25 mM HEPES pH 7.0, 500 mM NaCl, 5% Glycerol, 2 mM DTT, and 0.025% Azide